HHS Public Access

Author manuscript

NMR Biomed. Author manuscript; available in PMC 2019 May 01.

Published in final edited form as:

NMR Biomed. 2018 May ; 31(5): e3910. doi:10.1002/nbm.3910.

Neonatal Hyperglycemia Alters the Neurochemical Profile, Dendritic Arborization and Gene Expression in the Developing Rat Hippocampus

Raghavendra Rao[1,3,*], **Motaz Nashawaty**[1], **Saher Fatima**[1], **Kathleen Ennis**[1], and **Ivan Tkac**[2]

[1]Division of Neonatology, Department of Pediatrics, University of Minnesota

[2]Center for Magnetic Resonance Research, University of Minnesota

[3]Centre for Neurobehavioral Development, University of Minnesota

Abstract

Hyperglycemia (blood glucose concentration >150 mg/dL) is common in extremely low gestational age newborns (ELGAN; birth at <28 week gestation). Hyperglycemia increases the risk of brain injury in the neonatal period. The long-term effects are not well understood. In adult rats, hyperglycemia alters hippocampal energy metabolism. The effects of hyperglycemia on the developing hippocampus were studied in rat pups. In experiment 1, recurrent hyperglycemia of graded severity (moderate hyperglycemia: mean blood glucose, 214.6 ± 11.6 mg/dL; severe hyperglycemia, 338.9±21.7 mg/dL; control, 137.7 ± 2.6 mg/dL) was induced from postnatal day (P) 3 to P12. On P30, hippocampal neurochemical profile was determined using *in vivo* ^{1}H MR spectroscopy. Dendritic arborization in the hippocampal CA1 region was determined using microtubule-associated protein (MAP)-2 immunohistochemistry. In experiment 2, continuous hyperglycemia (mean blood glucose, 275.3 ± 25.8 mg/dL; control, 142.3 ± 2.6 mg/dL) was induced from P2 to P6 by injecting streptozotocin on P2. The mRNA expression of glycogen synthase 1 (*Gys1*), lactate dehydrogenase (*Ldh*), glucose transporter 1 (*Glut1*) and 3 (*Glut3*), and monocarboxylate transporter 1 (*Mct1*), 2 (*Mct2*) and 4 (*Mct4*) in the hippocampus was determined on P6. In experiment 1, MRS demonstrated lower lactate concentration and glutamate/glutamine ratio in the severe hyperglycemia group, compared with the control group ($p < 0.05$). PCr/Cr ratio was higher in both hyperglycemia groups ($p < 0.05$). MAP-2 histochemistry demonstrated longer apical segment length indicating abnormal synaptic efficacy in both hyperglycemia groups ($p < 0.05$). Experiment 2 showed lower *Glut1*, *Gys1* and *Mct4* expression, and higher *Mct1* expression in the hyperglycemia group, relative to the control group ($p < 0.05$). These results suggest that hyperglycemia alters substrate transport, lactate homeostasis, dendritogenesis and glutamate/glutamine cycling in the developing hippocampus. Abnormal neurochemical profile and dendritic structure due to hyperglycemia may partially explain the long-term hippocampus-mediated cognitive deficits in human ELGAN.

GRAPHICAL ABSTRACT

[*]Address for correspondence: Mayo Mail Code 39, 420 Delaware Street, SE, Minneapolis, MN 55455 (USA). Phone: 612-625-3260; Fax: 612-624-8176; raghurao@umn.edu.

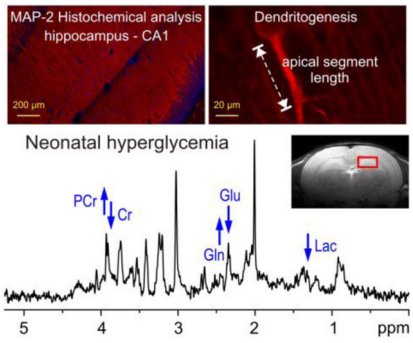

In vivo ^{1}H MR spectroscopy shows that recurrent neonatal hyperglycemia leads to lower lactate and glutamate/glutamine ratio, and higher phospho-creatine/creatine ratio in the developing rat hippocampus. Histochemical analysis demonstrates longer apical dendritic length, indicating decreased synaptic efficacy in the formerly hyperglycemic hippocampus. Altered monocarboxylate and glucose transporter expression in the hippocampus during neonatal hyperglycemia suggests that decreased lactate availability during development may be responsible for the long-term neurochemical and structural changes.

Keywords

Dendrite; hippocampus; hyperglycemia; lactate; MR spectroscopy; neonate; neurochemical profile; rat

INTRODUCTION

Hyperglycemia, defined as blood glucose concentration >150 mg/dl (>8.3 mmol/L) occurs in 40–80% of extremely low gestational age newborns (ELGAN; birth before 28 weeks of gestation)[1, 2]. Hyperglycemia begins soon after birth and persists for days to weeks. Relative hypoinsulinism combined with an inability to suppress endogenous glucose production during dextrose infusion is responsible for hyperglycemia in the ELGAN. Hyperglycemia is associated with mortality, severe intraventricular hemorrhage, sepsis and retinopathy of prematurity in the neonatal period[3–5]. The long-term effects on the brain are less well understood. Limited data demonstrate that neonatal hyperglycemia in ELGAN is associated with white matter reduction at term age[5], and a smaller head circumference and abnormal neurodevelopment at 2 years corrected age[2, 4]. The deleterious effects correlate with the severity and duration of hyperglycemia in the neonatal period[2, 4].

Abnormal hippocampal development and hippocampus-mediated cognitive deficits that persist into young adulthood are common in ELGAN[6, 7]. Whether hyperglycemia has a role in the structural and functional deficits is not known. Hippocampal injury is common in other causes of early-life hyperglycemia, for example, in children with early-onset type 1 diabetes[8]. Hippocampal development spans prenatal and postnatal periods with the peak development occurring postnatally[9]. A similar developmental trajectory is present in rats. Peak hippocampal development occurs during the first postnatal month and is characterized by active dendritogenesis, increased neuronal activity and energy requirement[9–11]. Insults

during this period lead to abnormal neurochemical profile, impaired dendritogenesis and long-term hippocampal dysfunction[10, 12, 13].

Previous studies from our lab and other labs have demonstrated that recurrent hyperglycemia during the first two postnatal weeks causes oxidative stress, DNA damage, inflammation and microgliosis in the cerebral cortex and hippocampus of rats[14, 15]. Oxidative stress and inflammation may negatively influence hippocampal dendritogenesis and function. Furthermore, in adult rats, hyperglycemia alters glycogen and lactate metabolism in the hippocampus[16, 17]. Astrocytic glycogen breakdown and astrocyte-neuron-lactate transport has an important role in hippocampal synaptic morphology and plasticity[18–20].

The objective of the present study was to determine the long-term effects of recurrent neonatal hyperglycemia of graded severity on hippocampal neurochemical profile and dendritic structure in rats. We used ultra-high-field (9.4T) *in vivo* ^{1}H MR spectroscopy (MRS) to determine hippocampal neurochemical profile. As we have previously demonstrated, *in vivo* ^{1}H MRS is a suitable method for assessing the long-term effects of an adverse perinatal condition on the developing hippocampus[13, 21]. We used microtubule-associated protein-2 (MAP-2) histochemical analysis to characterize dendritic architecture in the CA1 region of the hippocampus. MAP-2 is highly compartmentalized in the neuronal body and dendrites and thus useful for determining dendritic growth and branching[12]. Abnormal energy metabolism during peak dendritogenesis alters dendritic morphology that is characterized by a longer apical segment length (the length between neuronal soma and the initial branch point), fewer branches and impaired hippocampal plasticity[12, 22]. Based on the evidence of altered glycogen and lactate metabolism reported in adult rats with hyperglycemia[16, 17], we determined the effects of hyperglycemia on the mRNA expression of glycogen synthase 1 (*Gys1*) and lactate dehydrogenase (*Ldh*), the enzymes responsible for glycogen synthesis and lactate production, respectively, and selected glucose transporters (GLUT; *Glut1* and *Glut3*) and monocarboxylate transporters (MCT; *Mct1*, *Mct2* and *Mct4*) in the hippocampus. GLUT1 is the primary glucose transporter at the blood brain barrier (BBB) and astrocytes, while GLUT3 is the primary neuronal glucose transporter[23, 24]. MCT1 is the monocarboxylate transporter at BBB and astrocytes, while MCT2 is responsible for lactate import into neurons[24]. MCT4 is primarily expressed in astrocytes and is responsible for lactate efflux into the extracellular space for neuronal uptake via MCT2[18, 19]. We hypothesized that neonatal hyperglycemia would impair hippocampal development and lead to long-term neurochemical and structural alterations and that these impairments would vary by the severity of hyperglycemia.

EXPERIMENATAL DETAILS

Subjects

Male and female Sprague Dawley rat pups were used in the experiments. Pregnant dams were purchased (Harlan-Teklad, Indianapolis, IN) and allowed to deliver spontaneously. Litter size was limited to 8 pups (equal number of males and females) by random culling on postnatal day (P) 2. Pups were weaned on P21 and grouped in sets of 4 rats of same sex in a cage to ensure social interaction. Animals were maintained under standard laboratory conditions with free access to food and water and 12-hour light/dark cycle (lights on at

06:00 hr). Experiments were performed according to the National Institutes of Health guidelines. The Institutional Animal Care and Use Committee at University of Minnesota approved all experimental protocols.

Overall Design

Two non-overlapping experiments were performed. In Experiment 1, the long-term effects of recurrent hyperglycemia of graded severity on hippocampal neurochemical profile and dendritic arborization were determined at P30 using *in vivo* ^{1}H MRS and histochemical analysis. In Experiment 2, the acute effects of continuous hyperglycemia on mRNA expression of a select group of genes in the hippocampus were determined using quantitative polymerase chain reaction (qPCR) at P6. Both animal models cause transient hyperglycemia during the period of peak hippocampal development and simulate the condition in human preterm infants. Hyperglycemia is typically intermittent in ELGAN[1] due to the practice of insulin administration when blood glucose concentration exceeds predetermined thresholds[25]. However, there is a wide variation among the clinicians in the criteria used for insulin therapy and the target blood glucose ranges[26], leading to continuous hyperglycemia in many infants. Published and unpublished studies from our laboratory and other laboratories[14, 15] demonstrate that the two hyperglycemia models have similar adverse effects (oxidative stress and inflammation) on the brain regions.

Experiment 1

Induction of Recurrent Hyperglycemia—Rat pups in each litter were randomly assigned to the control (P30-Control group), moderate hyperglycemia (Moderate-HG group) and severe hyperglycemia (Severe-HG group) groups. Pups assigned to the hyperglycemia groups were subjected to hyperglycemia twice a day at 08:00 hr and 16:00 hr for 10 consecutive days (20 hyperglycemia episodes in total) from P3 to P12 using previously described method[14, 15]. These postnatal ages were chosen because of their similarity to the stage of hippocampal development in the ELGAN (P3) and full-term (P12) human infant, respectively[9, 27]. Pups were separated from the dams, weighed and subcutaneously injected with 30% dextrose (3 mg/g body weight; Moderate-HG group) or 50% dextrose (5 mg/g body weight; Severe-HG group). Dextrose injections were repeated one hour later using half the original dose (1.5 mg/g of 30% dextrose for Moderate-HG group and 2.5 mg/g of 50% dextrose for Severe-HG group). The volume of injection was 0.01 mL/g for the first injection and 0.005 mL/g for the second injection. Our previous study has demonstrated that this model induces hyperglycemia, beginning at 5 min after the first dextrose injection, with spontaneous resolution 120 min later[14], likely due to stimulation of insulin secretion from the pancreas. Pups assigned to the P30-Control group were subcutaneously injected with an equivalent volume of normal saline at the corresponding times. Pups were kept separated from their dams for 120 min and maintained at an ambient temperature of 34°C (nesting temperature). Blood glucose concentration was measured from representative rats from each group (N = 4–6 per group) during each episode of hyperglycemia. After the termination of recurrent hyperglycemia on P12, blood glucose was determined on P20 and P27 in representative rats from the three groups (N = 7 per group) to confirm the absence of new-onset hyperglycemia in the two formerly hyperglycemia groups.

In vivo ^{1}H MR Spectroscopy—^{1}H MRS data were acquired on P30, which neurodevelopmentally corresponds to a young human child[27]. ^{1}H MR spectra were collected from spontaneously breathing pups (N = 6–7 per group) under inhalational anesthesia (isoflurane, 3% for induction and 1–2% for maintenance in a 50:50 mixture of N_2O and O_2) using previously published protocol[28, 29]. All MRI and ^{1}H MRS experiments were performed using a 9.4T/31cm horizontal bore magnet (Varian/Magnex Scientific; Yarnton, UK) equipped with a 15-cm gradient/shim coil (Resonance Research, Inc., Billerica, MA, USA) and interfaced to a DirectDrive console (Agilent/Varian; Palo Alto, CA). Uniform temperature was maintained inside the magnet using circulating warm water in tubes surrounding the cradle containing the animal. The depth of anesthesia was monitored using continuous respiratory rate monitoring. Multi-slice fast spin-echo (FSE) MR imaging in axial and sagittal orientation (slice thickness = 1 mm) was used for precise positioning of the 8 μl volume of interest (VOI = 2.5 × 1.3 × 2.5 mm^3) centered in the left dorsal hippocampus. The B_0 magnetic field homogeneity was adjusted by FASTMAP shimming[30]. *In vivo* ^{1}H MRS data were acquired using ultra-short echo-time STEAM (TE = 2 ms, TR = 5 s) localization sequence combined with VAPOR water suppression[31]. Metabolites were quantified using LCModel with the spectrum of fast relaxing macromolecules acquired *in vivo* included in the basis set. Only metabolites that were consistently quantified with the Cramèr-Rao lower bounds below 50% were included for the further analysis. The unsuppressed water signal was used as an internal reference, assuming 80% brain water content.

Histochemical Analysis

Tissue Preparation: Immediately following the MRI/MRS experiment, the rat was deeply anesthetized using an overdose of sodium pentobarbital (100 mg/kg, ip.). After *in situ* transcardial perfusion-fixation (normal saline, followed by 5% formaldehyde and 5% sucrose in phosphate-buffered saline), the brain was removed and processed for histochemistry using previously described methods[12, 32]. Coronal brain sections (20 μm thickness) were obtained using a cryostat (Model CM 1950, Leica Instruments GmbH, Nussloch, Germany), mounted on glass slides and stored at −20 °C until immunohistochemistry.

MAP-2 Immunohistochemistry: Dendritic morphology in the hippocampus was assessed using MAP-2 histochemical analysis as in our previous study[12]. Brain sections corresponding to 0.8 mm to 2.6 mm anterior to the interaural line in an age-appropriate rat brain atlas[33] were used (N = 6 per group; 4 brain sections per rat). This region corresponds to the placement of the VOI on ^{1}H-MRS. Brain sections were incubated overnight with anti-MAP2 primary antibody (1:100; MAB3418; MilliporeSigma; Billerica, MA) at 4°C, followed by incubation with the Alexa Fluor 555 secondary antibody (1:200; Thermo Fisher Scientific; Waltham, MA) for 2 hr at room temperature. Sections were mounted using a fluorescence media containing DAPI and stored at 4°C.

MAP-2 Histochemical Analysis: MAP-2 stained brain sections were visualized using a microscope and FITC, RHOD, and DAPI filters (DM6 B; Leica, Wetzlar, Germany) at a magnification of ×100–1000. Digital photomicrographs were obtained using a digital camera

(DFC7000 T; Leica) and projected on to the computer screen using a software program (LAS X; Leica). The length of the dendritic segment from pyramidal neuron soma to the first branch point (apical segment length) of five randomly chosen dendrites in the hippocampal CA1 region was measured as previously described[12, 22]. Only dendrites in which the first lateral branching was unambiguously present in the field of observation were used for quantification. The mean apical segment length in each animal was determined and group means were determined.

Immunohistochemical Analysis for Astrocytosis: Astrocytosis in the hippocampus was determined by staining the brain sections (N = 6 per group) for anti-S100b protein (1:200, ab4066; Abcam; Cambridge, MA). All S-100b-positive cells in the hippocampus were counted using a software program (ImageJ; NIH; Bethesda, MA) as previously described[14] and group means were determined.

Experiment 2

Induction of Hypoinsulinemic Hyperglycemia—Hypoinsulinemic hyperglycemia was induced by injecting rat pups with streptozotocin (STZ) in a dose of 100 mg/kg ip on P2. Neonatal STZ rodent model is a well-established model for studying the effects of neonatal hyperglycemia[34]. Unlike adult rats, where STZ administration causes permanent destruction of pancreatic β cells and results in permanent hyperglycemia, STZ administration on P2 causes transient hyperglycemia that lasts until P6[34]. Unpublished data from our laboratory demonstrates that this model is associated with abnormal hippocampal dendritogenesis and function at adulthood. Littermates in the control group (P6-Control group) were administered citrate buffer of equivalent volume. Blood glucose concentration was measured daily in the two groups.

Determination of Transcript Expression

Tissue Preparation: Pups in the P6-Control and STZ groups were killed on P6 by administering pentobarbital (100 mg/kg ip.). The brain was removed and hippocampus was rapidly dissected on ice, flash-frozen using liquid nitrogen and stored at −80C until analysis.

Quantitative Polymerase Chain Reaction (qPCR): The mRNA expression of glycogen synthase 1 (*Gys1*), lactate dehydrogenase (*Ldh*), glucose transporters *Glut1* and *Glut3,* and monocarboxylate transporters *Mct1*, *Mct2* and *Mct4* in the hippocampus of P6-Control and STZ groups was determined using FastStart Universal Probe Master (Sigma Aldrich, St. Louis, MO) and TaqMan® gene expression probes (Life Technologies, Carlsbad, CA) using previously described methods from our lab[14]. Samples (N = 8 per group) were assayed in duplicate. Data were normalized against the P6-Control group and group means were determined.

Statistical Analysis

The effect of hyperglycemia on blood glucose concentration, neurochemical profile and the apical segment length in Experiment 1 were determined using ANOVA. Intergroup differences were determined using two-tailed Bonferroni-adjusted unpaired *t* tests. The effect of hyperglycemia on mRNA expression in Experiment 2 was determined using two-

tailed unpaired *t* tests. Values are reported as mean ± SD for MRS results and mean ± SEM for the rest. Statistical significance was set at $p < 0.05$.

RESULTS

Experiment 1

Blood Glucose Concentration and Body Weight—Blood glucose concentration during the two hours after the dextrose injection were higher in the Moderate-HG group and Severe-HG group, relative to the P30-Control group: P30-Control group, 137.7 ± 2.6 mg/dL; Moderate-HG group, 214.6 ± 11.6 mg/dL; Severe-HG group, 338.9±21.7 mg/dL; $p<0.001$ (ANOVA) and $p<0.001$, intergroup differences (Bonferroni adjusted *t* tests). The blood glucose concentration 3 hours after the first dextrose bolus was comparable in the three groups: P30-Control group: 133.8 ± 5.3 mg/dL; Moderate-HG group: 128.4 ± 8.1 mg/dL; Severe-HG group: 147.2 ± 19.5 mg/dL; p = NS. There were no differences in mean blood glucose concentration among the 20 hypoglycemia episodes from P3 to P12. After the termination of recurrent hyperglycemia on P12, blood glucose concentrations were determined on P20 and P27 to confirm the absence of new-onset hyperglycemia in the two formerly hyperglycemia groups. The three groups had comparable blood glucose concentration on P20 and P27 (Supplemental Table). The body weights on P30 were comparable in the three groups: P30-Control group, 107 ± 3.6 g; Moderate-HG, 106 ± 2.8 g; Severe-HG, 102 ± 3.9 g; p = NS.

In vivo ^{1}H MR Spectroscopy—Representative ^{1}H MR spectra from the control group and the two hyperglycemia groups are shown in Figure 1. The spectral quality, routinely achieved in this study (FWHM = 4.4 ± 1.1 Hz and SNR = 14.1 ± 2.4 (mean ± SD) from the default LCModel output), allowed reliable quantification of 17 brain metabolites, including: alanine (Ala), ascorbate (Asc), aspartate (Asp), creatine (Cr), phosphocreatine (PCr), γ-aminobutyric acid (GABA), glucose (Glc), glutamine (Gln), glutamate (Glu), glutathione (GSH), *myo*-inositol (Ins), lactate (Lac), *N*-acetylaspartate (NAA), *N*-acetylaspartylglutamate (NAAG), phosphoethanolamine (PE), taurine (Tau), glycerophosphocholine+phosphocholine (GPC+PC) and of underlying macromolecules (MM). In addition, PCr/Cr and Glu/Gln concentration ratios were determined.

Relative to the P30-Control group, Lac concentration (−31%; p = 0.03) and Glu/Gln ratio (−18%; p = 0.04) were lower in the Severe-HG group (Figure 2). PCr/Cr ratio was higher in the Moderate-HG (+18%; p = 0.03) and Severe-HG (+18%; p = 0.04) groups, compared with the P30-Control group ($p < 0.05$; Figure 2). No other metabolites were altered.

Histochemical Analysis: Figure 3 shows MAP-2 stained hippocampal sections from a rat in the P30-Control group (Figure 3a) with the apical segment length of a CA1 pyramidal neuron highlighted (Figure 3b). There was a main effect of group on the apical segment length of the dendrites ($p < 0.001$; ANOVA). Compared with the P30-Control group, the apical segment length was longer in the two hyperglycemia groups ($p < 0.01$, Figure 3c). A graded effect (Severe-HG group > Moderate-HG group > P30-Control group, $p < 0.05$) was present (Figure 3c). The effect of antecedent hyperglycemia on astrocytosis in the hippocampus was also determined (Supplemental Figure**, online**). Comparable number of

astrocytes were present in the three groups: P30-Control group: 49 ± 5/mm^2; Moderate-HG group: 53 ± 2/mm^2; Severe-HG: 54 ± 3/mm^2; p = NS.

Experiment 2

Blood Glucose Concentration—Beginning at 24 hours after the STZ injection and until tissue harvest on P6 (i.e., from P3 to P6), the mean blood glucose concentration was higher in the STZ group, relative to the P6-Control group: P6-Control group: 137.5 ± 3.7 mg/dL; STZ group: 180.9 ± 33.8 mg/dL; $p < 0.01$ on P3; and P6-Control group: 145.5 ± 3.1 mg/dL; STZ group: 267.5 ± 51.9 mg/dL; $p < 0.05$ on P6.

mRNA Expression—The effect of hyperglycemia on hippocampal mRNA expression on P6 is shown in Figure 4. Relative to the P6-Control group, *Glut1* (−19%), *Gys1* (−22%) and *Mct4* (−29%) expression was lower, and *Mct1* (+38%) expression was higher in the STZ group ($p < 0.05$; Figure 4). *Ldh*, *Mct2* (Figure 4) and *Glut3* (not shown) expression was not altered.

DISCUSSION

The present study demonstrates that hyperglycemia comparable in severity to that seen in human ELGAN alters the neurochemical profile, dendritic structure and gene expression in the hippocampus of developing rats. The observed changes suggest altered substrate transport, energy metabolism, lactate homeostasis, dendritogenesis and glutamate-glutamine cycling in the hippocampus exposed to hyperglycemia. The neurochemical and structural changes were observed two weeks after the hyperglycemia episodes had ceased, suggesting that they represent long-term sequelae of neonatal hyperglycemia. These results may partially explain the long-term hippocampal structural and functional deficits reported in the human ELGAN infants[2, 4, 5].

The neurochemical profiling (Figure 2) at P30 revealed lower Lac concentration in the hippocampus of formerly hyperglycemic rats. A similar effect has been observed in the hyperglycemic fetal rabbit brain and has been attributed to the inhibitory effect of ketone bodies (β-hydroxybutyrate) on glycolysis and glucose utilization during hyperglycemia[35]. Altered glucose flux through the pyruvate carboxylase and pyruvate dehydrogenase pathways reported in the Lapidot and Haber study[35] may explain the lower Glu/Gln ratio in the present study. Although, the absolute increase in Gln concentration (0.25 μmol/g) was smaller than the decrease in Glu (0.65 μmol/g) in the Severe-HG group, the relative changes in Gln (11% increase) likely had a greater impact than the change in Glu (7% decrease) for the lower Glu/Gln ratio. Loss of neurons (where Glu is predominantly localized) and/or increased number of astrocytes (where Gln is predominantly localized) is unlikely to explain the lower Glu/Gln ratio. The hyperglycemia model used in the present study is not associated with neuronal loss[14]. Unchanged NAA levels, the marker of neuronal integrity (Figure 2), and unchanged astrocyte number (Supplemental Figure) in the hyperglycemia groups also rule out neuronal loss and/or astrocytosis as the explanation for decreased Glu/Gln ratio. The increase in the PCr/Cr ratio in the two hyperglycemia groups likely indicates lower demands for ATP and PCr, secondary to decreased neuronal activity, as has been observed in rodent models of ethanol intoxication and hibernation[36, 37]. Equivalent

changes in PCr (8% increase) and Cr (8% decrease) were responsible for the increased PCr/Cr ratio in both hyperglycemia groups (Figure 2). This is not surprising given that PCr and Cr in equilibrium (1:1) under steady state, and altered energy metabolism leads to reciprocal and equivalent changes in PCr and Cr concentrations in the hippocampus[38]. Lower Lac levels (and a trend for lower Glu levels; Figure 2) in the Severe-HG group corroborate decreased neuronal activity, since previous studies in humans reveal that increased brain activity is accompanied by increased Lac and Glu levels[39, 40]. Dendrites with elongated apical segment length in the hyperglycemia groups also support suppressed neuronal activity in the hippocampus. Longer apical segment length reflects immature dendritogenesis and is associated with impaired hippocampal plasticity and function[12].

Altered expression of genes associated with substrate transport in the hippocampus of hyperglycemic P6 rats in Experiment 2 provide potential explanation for the underpinnings of the neurochemical and structural effects observed at P30 in Experiment 1. The expression of four of the seven targeted genes was altered in the STZ group. Decreased *Glut1* expression in the STZ group (Figure 4) most likely represents astrocyte-specific GLUT1 changes. Astrocyte GLUT1 expression increases progressively from birth and thus amenable to alteration, whereas the BBB GLUT1 expression remains low until P10[41, 42]. Lack of changes in the expression of neuronal glucose transporter *Glut3* is not surprising given that GLUT3 expression in hippocampus is low until P10 and increases only after P14[41, 42], i.e., beyond the period of hyperglycemia in the present study. The lower expression of *Gsy1*, the enzyme responsible for glycogen synthesis in astrocytes supports decreased astrocytic glucose uptake and storage and is consistent with a previous report of decreased glycogen concentration in the developing brain during hyperglycemia[43].

Upregulation of *Mct1* responsible for lactate and ketone body transport across the BBB and astrocytes[24] in the STZ-group may be a compensatory response to decreased glucose availability, secondary to *Glut1* suppression. Although glucose is its primary energy substrate, the developing brain is capable of maintaining energy production using ketone bodies[44, 45]. The expression of *Mct2*, responsible for neuronal lactate uptake was not altered. However, the expression of *Mct4*, responsible for lactate efflux from astrocytes was suppressed in the STZ group (Figure 4). Collectively, these results suggest a shift in substrate transport and altered lactate homeostasis in the hippocampus.

The results also demonstrate that hyperglycemia has disparate effects on substrate transport and metabolism in the developing and mature hippocampi. In adult rats, hyperglycemia is associated with increased glycogen concentration and decreased MCT2 protein expression in the hippocampus[16, 17]. MCT4 expression is not altered[16]. The effect on GLUT1 has been inconsistent with some studies reporting upregulation and others finding no alteration[46, 47]. Similar to the results of the present study, MCT1 expression is upregulated and GLUT3 expression remains unaltered in the mature hippocampus[23, 48]. Despite these age-related differences, the end result of exposure to hyperglycemia appears to be similar in the two age groups, namely, decreased lactate availability to neurons, secondary to MCT2 suppression in the adult hippocampus[16], and decreased astrocytic lactate production and efflux due to GLUT1, glycogen synthase and MCT4 suppression (Figure 4) in the developing hippocampus.

As astrocyte-neuron lactate transport is essential for hippocampal synaptogenesis and plasticity[18, 19], decreased lactate availability during the period of active dendritogenesis may have led to the abnormal dendritic arborization observed in Experiment 1. However, without concurrent MRS, transcript and histochemical analyses in the same animals, this possibility remains conjectural. It is also possible that performing MRS on P6 during the period of hyperglycemia may have uncovered additional neurochemical changes than those observed on P30. MRS in animal models of perinatal brain injury typically demonstrates more neurochemical changes in the hippocampus during the acute phase than assessment at a later time point because of the brain plasticity during development[13, 21, 29]. Finally, without additional behavioral and cognitive tests, the functional relevance of the observed neurochemical, gene and structural changes cannot be determined.

In summary, this preclinical study demonstrates that neonatal hyperglycemia alters substrate transporter expression and leads to long-term abnormalities in neurochemistry and dendritic structure in the developing hippocampus. These results may partially explain the hippocampal structural and functional impairments in the human ELGAN[2, 4, 5].

Supplementary Material

Refer to Web version on PubMed Central for supplementary material.

Acknowledgements

The authors thank Sharlotte Irwin and Jun Chen for their assistance with the qPCR experiments. Funded by the Viking Children's Fund, Department of Pediatrics, University of Minnesota (Grant Number: 1701-11857-21792-1726331). The Center for Magnetic Resonance Research at the University of Minnesota is supported by NIH grants P41 EB015894 and P30 NS076408.

Abbreviations:

Ala	alanine
Asc	ascorbate
Asp	aspartate
BBB	blood brain barrier
Cr	creatine
ELGAN	extremely low gestational age neonate
FSE	fast spin-echo
GABA	γ-aminobutyric acid
Glc	glucose
GLUT	glucose transporter
Gln	glutamine

Glu	glutamate
GSH	glutathione
GPC	glycerophosphocholine
Gsy1	glycogen synthase 1
HG	hyperglycemia
Ins	*myo*-inositol
Lac	lactate
Ldh	lactate dehydrogenase
MCT	monocarboxylate transporter
MM	macromolecules
MRS	MR spectroscopy
NAA	*N*-acetylaspartate
NAAG	*N*-acetylaspartylglutamate
NT	number of transients
PC	phosphocholine
PCr	phosphocreatine
PE	phosphoethanolamine
P	postnatal day
qPCR	quantitative polymerase chain reaction
STZ	streptozotocin
Tau	taurine
TE	echo time
TR	repetition time
VOI	volume of interest

References

1. Beardsall K, Vanhaesebrouck S, Ogilvy-Stuart AL, Vanhole C, Palmer CR, Ong K, vanWeissenbruch M, Midgley P, Thompson M, Thio M, Cornette L, Ossuetta I, Iglesias I, Theyskens C, de Jong M, Gill B, Ahluwalia JS, de Zegher F, Dunger DB. Prevalence and determinants of hyperglycemia in very low birth weight infants: cohort analyses of the NIRTURE study. J Pediatr 2010;157(5):715–719. [PubMed: 20570286]

2. Ramel SE, Long JD, Gray H, Durrwachter-Erno K, Demerath EW, Rao R. Neonatal hyperglycemia and diminished long-term growth in very low birth weight preterm infants. J Perinatol 2013;33(11): 882–886. [PubMed: 23846492]

3. Hays SP, Smith EO, Sunehag AL. Hyperglycemia is a risk factor for early death and morbidity in extremely low birth-weight infants. Pediatrics 2006;118(5):1811–1818. [PubMed: 17079549]

4. van der Lugt NM, Smits-Wintjens VE, van Zwieten PH, Walther FJ. Short and long term outcome of neonatal hyperglycemia in very preterm infants: a retrospective follow-up study. BMC Pediatr 2010;10:52. [PubMed: 20646308]

5. Alexandrou G, Skiold B, Karlen J, Tessma MK, Norman M, Aden U, Vanpee M. Early hyperglycemia is a risk factor for death and white matter reduction in preterm infants. Pediatrics 2010;125(3):e584–591. [PubMed: 20176674]

6. Aanes S, Bjuland KJ, Skranes J, Lohaugen GC. Memory function and hippocampal volumes in preterm born very-low-birth-weight (VLBW) young adults. Neuroimage 2015;105:76–83. [PubMed: 25451477]

7. Nosarti C, Froudist-Walsh S. Alterations in development of hippocampal and cortical memory mechanisms following very preterm birth. Dev Med Child Neurol 2016;58 Suppl 4:35–45. [PubMed: 27027606]

8. Ho MS, Weller NJ, Ives FJ, Carne CL, Murray K, Vanden Driesen RI, Nguyen TP, Robins PD, Bulsara M, Davis EA, Jones TW. Prevalence of structural central nervous system abnormalities in early-onset type 1 diabetes mellitus. J Pediatr 2008;153(3):385–390. [PubMed: 18534238]

9. Avishai-Eliner S, Brunson KL, Sandman CA, Baram TZ. Stressed-out, or in (utero)? Trends Neurosci 2002;25(10):518–524. [PubMed: 12220880]

10. Fretham SJ, Carlson ES, Georgieff MK. The role of iron in learning and memory. Adv Nutr 2011;2(2):112–121. [PubMed: 22332040]

11. Nehlig A Cerebral energy metabolism, glucose transport and blood flow: changes with maturation and adaptation to hypoglycaemia. Diabetes Metab 1997;23(1):18–29. [PubMed: 9059763]

12. Raman L, Hamilton KL, Gewirtz JC, Rao R. Effects of chronic hypoxia in developing rats on dendritic morphology of the CA1 subarea of the hippocampus and on fear-potentiated startle. Brain Res 2008;1190:167–174. [PubMed: 18083146]

13. Rao R, Tkac I, Schmidt AT, Georgieff MK. Fetal and neonatal iron deficiency causes volume loss and alters the neurochemical profile of the adult rat hippocampus. Nutr Neurosci 2011;14(2):59–65. [PubMed: 21605501]

14. Gisslen T, Ennis K, Bhandari V, Rao R. Recurrent hypoinsulinemic hyperglycemia in neonatal rats increases PARP-1 and NF-kappaB expression and leads to microglial activation in the cerebral cortex. Pediatr Res 2015;78(5):513–519. [PubMed: 26200703]

15. Tayman C, Yis U, Hirfanoglu I, Oztekin O, Goktas G, Bilgin BC. Effects of hyperglycemia on the developing brain in newborns. Pediatr Neurol 2014;51(2):239–245. [PubMed: 24950664]

16. Shima T, Jesmin S, Matsui T, Soya M, Soya H. Differential effects of type 2 diabetes on brain glycometabolism in rats: focus on glycogen and monocarboxylate transporter 2. J Physiol Sci 2018;68(1):69–75. [PubMed: 27987117]

17. Shima T, Matsui T, Jesmin S, Okamoto M, Soya M, Inoue K, Liu YF, Torres-Aleman I, McEwen BS, Soya H. Moderate exercise ameliorates dysregulated hippocampal glycometabolism and memory function in a rat model of type 2 diabetes. Diabetologia 2017;60(3):597–606. [PubMed: 27928614]

18. Suzuki A, Stern SA, Bozdagi O, Huntley GW, Walker RH, Magistretti PJ, Alberini CM. Astrocyte-neuron lactate transport is required for long-term memory formation. Cell 2011;144(5):810–823. [PubMed: 21376239]

19. Steinman MQ, Gao V, Alberini CM. The Role of Lactate-Mediated Metabolic Coupling between Astrocytes and Neurons in Long-Term Memory Formation. Front Integr Neurosci 2016;10:10. [PubMed: 26973477]

20. Bergersen LH. Lactate transport and signaling in the brain: potential therapeutic targets and roles in body-brain interaction. J Cereb Blood Flow Metab 2015;35(2):176–185. [PubMed: 25425080]

21. Rao R, Tkac I, Unger EL, Ennis K, Hurst A, Schallert T, Connor J, Felt B, Georgieff MK. Iron supplementation dose for perinatal iron deficiency differentially alters the neurochemistry of the frontal cortex and hippocampus in adult rats. Pediatr Res 2013;73(1):31–37. [PubMed: 23095980]
22. Jorgenson LA, Wobken JD, Georgieff MK. Perinatal iron deficiency alters apical dendritic growth in hippocampal CA1 pyramidal neurons. Dev Neurosci 2003;25(6):412–420. [PubMed: 14966382]
23. Simpson IA, Appel NM, Hokari M, Oki J, Holman GD, Maher F, Koehler-Stec EM, Vannucci SJ, Smith QR. Blood-brain barrier glucose transporter: effects of hypo- and hyperglycemiarevisited. J Neurochem 1999;72(1):238–247. [PubMed: 9886075]
24. Simpson IA, Carruthers A, Vannucci SJ. Supply and demand in cerebral energy metabolism: the role of nutrient transporters. J Cereb Blood Flow Metab 2007;27(11):1766–1791. [PubMed: 17579656]
25. Bottino M, Cowett RM, Sinclair JC. Interventions for treatment of neonatal hyperglycemia in very low birth weight infants. Cochrane Database Syst Rev 2011(10):CD007453. [PubMed: 21975769]
26. Alsweiler JM, Kuschel CA, Bloomfield FH. Survey of the management of neonatal hyperglycaemia in Australasia. J Paediatr Child Health 2007;43(9):632–635. [PubMed: 17608650]
27. Semple BD, Blomgren K, Gimlin K, Ferriero DM, Noble-Haeusslein LJ. Brain development in rodents and humans: Identifying benchmarks of maturation and vulnerability to injury across species. Prog Neurobiol 2013;106–107:1–16.
28. Tkac I, Rao R, Georgieff MK, Gruetter R. Developmental and regional changes in the neurochemical profile of the rat brain determined by in vivo 1H NMR spectroscopy. Magn Reson Med 2003;50(1):24–32. [PubMed: 12815675]
29. Rao R, Tkac I, Townsend EL, Gruetter R, Georgieff MK. Perinatal iron deficiency alters the neurochemical profile of the developing rat hippocampus. J Nutr 2003;133(10):3215–3221. [PubMed: 14519813]
30. Gruetter R, Tkac I. Field mapping without reference scan using asymmetric echo-planar techniques. Magn Reson Med 2000;43(2):319–323. [PubMed: 10680699]
31. Tkac I, Starcuk Z, Choi IY, Gruetter R. In vivo 1H NMR spectroscopy of rat brain at 1 ms echo time. Magn Reson Med 1999;41(4):649–656. [PubMed: 10332839]
32. Rao R, Tkac I, Townsend EL, Ennis K, Gruetter R, Georgieff MK. Perinatal iron deficiency predisposes the developing rat hippocampus to greater injury from mild to moderate hypoxia-ischemia. J Cereb Blood Flow Metab 2007;27(4):729–740. [PubMed: 16868555]
33. Sherwood NM, Timiras PS. A Steriotaxic Atlas of the Developing Rat Brain. Berkeley: University of California Press; 1970 1–209 p.
34. Portha B, Blondel O, Serradas P, McEvoy R, Giroix MH, Kergoat M, Bailbe D. The rat models of non-insulin dependent diabetes induced by neonatal streptozotocin. Diabete Metab 1989;15(2):61–75. [PubMed: 2525491]
35. Lapidot A, Haber S. Effect of endogenous beta-hydroxybutyrate on brain glucose metabolism in fetuses of diabetic rabbits, studied by (13)C magnetic resonance spectroscopy. Brain Res Dev Brain Res 2002;135(1–2):87–99. [PubMed: 11978397]
36. Denays R, Chao SL, Mathur-Devre R, Jeghers O, Fruhling J, Noel P, Ham HR. Metabolic changes in the rat brain after acute and chronic ethanol intoxication: a 31P NMR spectroscopy study. Magn Reson Med 1993;29(6):719–723. [PubMed: 8350714]
37. Henry PG, Russeth KP, Tkac I, Drewes LR, Andrews MT, Gruetter R. Brain energy metabolism and neurotransmission at near-freezing temperatures: in vivo (1)H MRS study of a hibernating mammal. J Neurochem 2007;101(6):1505–1515. [PubMed: 17437538]
38. Rao R, Ennis K, Long JD, Ugurbil K, Gruetter R, Tkac I. Neurochemical changes in the developing rat hippocampus during prolonged hypoglycemia. J Neurochem 2010;114(3):728–738. [PubMed: 20477939]
39. Mangia S, Tkac I, Gruetter R, Van de Moortele PF, Maraviglia B, Ugurbil K. Sustained neuronal activation raises oxidative metabolism to a new steady-state level: evidence from 1H NMR spectroscopy in the human visual cortex. J Cereb Blood Flow Metab 2007;27(5):1055–1063. [PubMed: 17033694]

40. Bednarik P, Tkac I, Giove F, DiNuzzo M, Deelchand DK, Emir UE, Eberly LE, Mangia S. Neurochemical and BOLD responses during neuronal activation measured in the human visual cortex at 7 Tesla. J Cereb Blood Flow Metab 2015;35(4):601–610. [PubMed: 25564236]
41. Vannucci SJ. Developmental expression of GLUT1 and GLUT3 glucose transporters in rat brain. J Neurochem 1994;62(1):240–246. [PubMed: 8263524]
42. Vannucci SJ, Clark RR, Koehler-Stec E, Li K, Smith CB, Davies P, Maher F, Simpson IA. Glucose transporter expression in brain: relationship to cerebral glucose utilization. Dev Neurosci 1998;20(4–5):369–379. [PubMed: 9778574]
43. Edwards C, Rogers KJ. Some factors influencing brain glycogen in the neonate chick. J Neurochem 1972;19(12):2759–2766. [PubMed: 4652628]
44. Nehlig A Respective roles of glucose and ketone bodies as substrates for cerebral energy metabolism in the suckling rat. Dev Neurosci 1996;18(5–6):426–433. [PubMed: 8940615]
45. Ennis K, Dotterman H, Stein A, Rao R. Hyperglycemia accentuates and ketonemia attenuates hypoglycemia-Induced neuronal injury in the developing rat brain. Pediatr Res 2014;77(1–1):84–90. [PubMed: 25279990]
46. Duelli R, Maurer MH, Staudt R, Heiland S, Duembgen L, Kuschinsky W. Increased cerebral glucose utilization and decreased glucose transporter Glut1 during chronic hyperglycemia in rat brain. Brain Res 2000;858(2):338–347. [PubMed: 10708685]
47. Nardin P, Zanotto C, Hansen F, Batassini C, Gasparin MS, Sesterheim P, Goncalves CA. Peripheral Levels of AGEs and Astrocyte Alterations in the Hippocampus of STZ-Diabetic Rats. Neurochem Res 2016;41(8):2006–2016. [PubMed: 27084774]
48. Canis M, Maurer MH, Kuschinsky W, Duembgen L, Duelli R. Increased densities of monocarboxylate transporter MCT1 after chronic hyperglycemia in rat brain. Brain Res 2009;1257:32–39. [PubMed: 19118535]

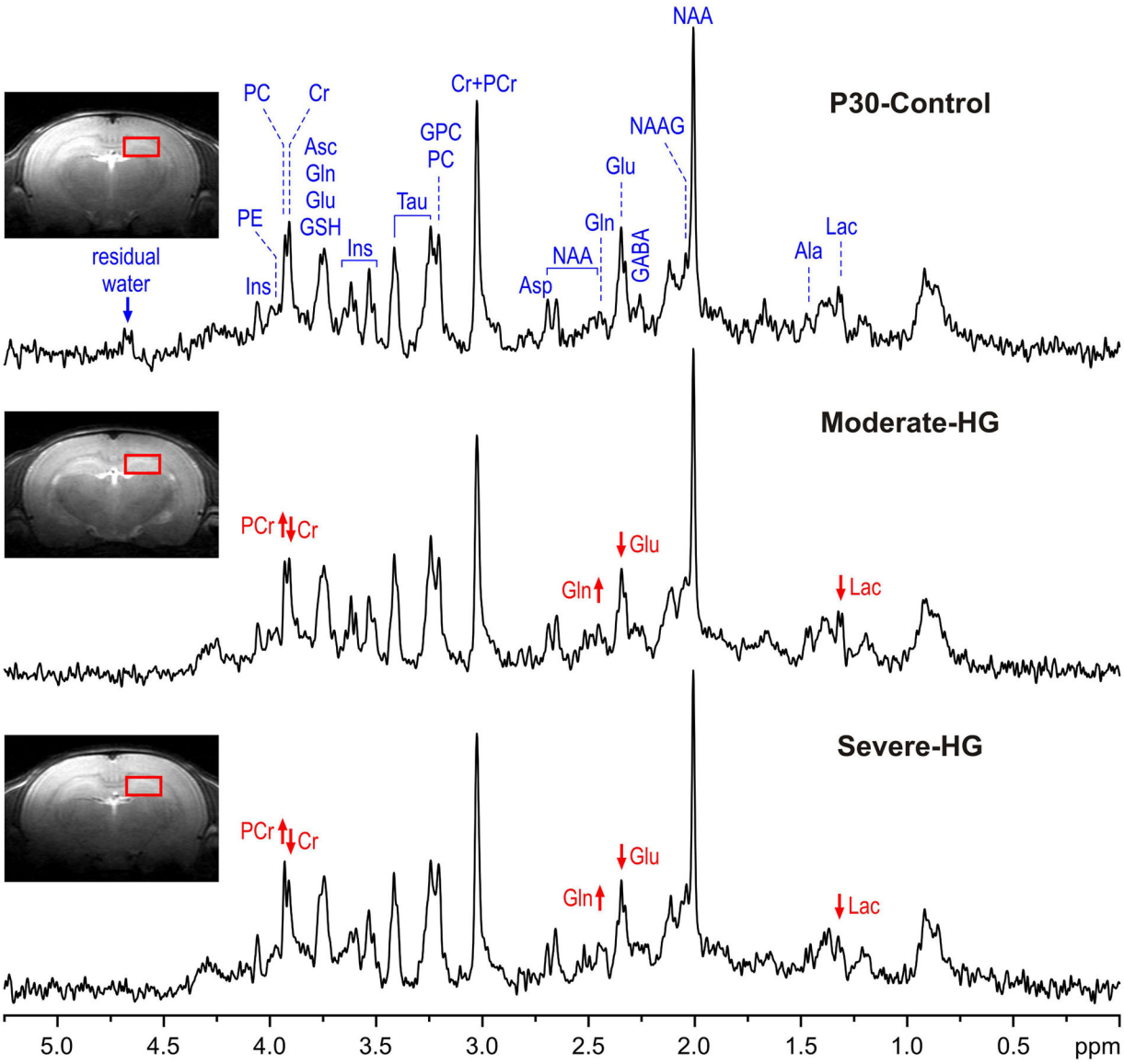

Figure 1.

Representative *in vivo* ^{1}H MR spectra acquired from the hippocampus of the control (P30-Control), moderate hyperglycemia (Moderate-HG) and severe hyperglycemia (Severe-HG)) rats at postnatal day 30 (STEAM, Te = 2 ms, TR = 5 s, NT = 240). Axial and sagittal FSE images show the typical selection of the 8 μl VOI in the dorsal hippocampus. Arrows show the direction of changes in creatine (Cr), phosphocretine (PCr), glutamine (Gln), glutamate (Glu) and lactate (Lac) in the two hyperglycemia groups, relative to the control group. Abbreviations: Ala, alanine; Asc, ascorbate; Asp, aspartate; GABA, γ-aminobutyric acid; GSH, glutathione; GPC, glycerophosphocholine; Ins, *myo*-inositol; Lac, lactate; NAA, *N*-acetylaspartate; NAAG, *N*-acetylaspartylglutamate; PC, phosphocholine; PE, phosphoethanolamine; Tau, taurine.

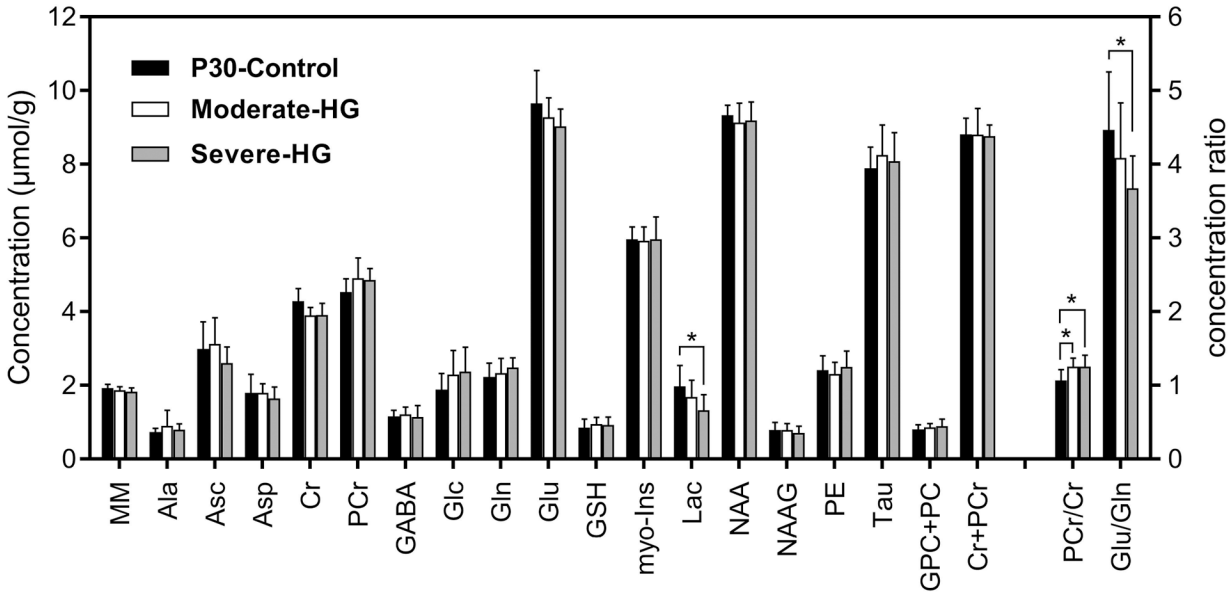

Figure 2.

Comparison of hippocampal neurochemical profiles of the control (P30-Control; black, N = 7), moderate hyperglycemia (Moderate-HG; white, N = 6) and severe hyperglycemia (Severe-HG; gray, N = 7) groups on postnatal day 30. Values are mean ± SD; t-test, *p < 0.05. Abbreviations: MM, macromolecules; Ala, alanine; Asc, ascorbate; Asp, aspartate; Cr, creatine: PCr, phosphocreatine; GABA, γ-aminobutyric acid: Glc, glucose; Gln, glutamine; Glu, glutamate; GSH, glutathione; Ins, *myo*-inositol; Lac, lactate; NAA, *N*-acetylaspartate; NAAG, *N*-acetylaspartylglutamate; PE, phosphoethanolamine; Tau, taurine; GPC+PC, glycerophosphocholine+phosphocholine; Cr+PCr, total creatine; PCr/Cr, phosphocreatine to creatine ratio; Glu/Gln, glutamate/glutamine ratio.

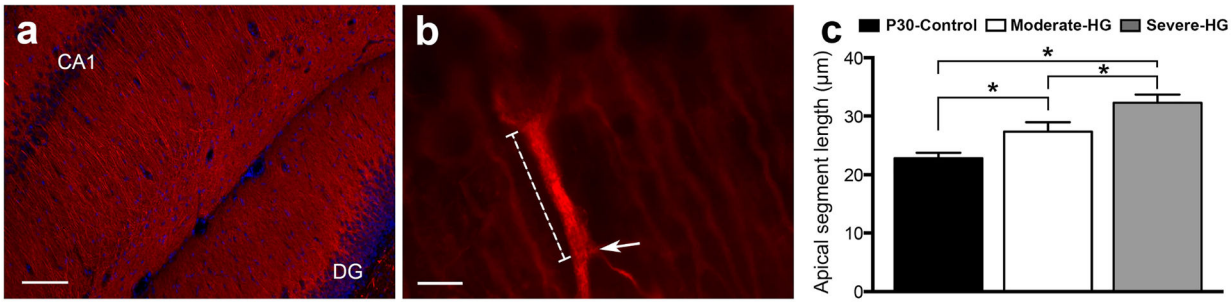

Figure 3.

Effect of antecedent hyperglycemia on dendritic arborization in the CA1 region of the hippocampus in rats on postnatal day 30. Photomicrographs of microtubule-associated protein-2 stained brain sections from a rat in the control group show dendritic architecture in the CA1 region of the hippocampus (**a**) and a dendrite with the first branching point (arrow) and apical segment length (dotted line) (**b**). (DG, dentate gyrus; bar in **a** = 200 μm and bar in **b** = 20 μm). **c**) Apical segment length in the control (P30-Control; black), moderate hyperglycemia (Moderate-HG; white) and severe hyperglycemia (Severe-HG; gray) groups. Values are mean ± SEM; N = 6 per group; *$p < 0.05$.

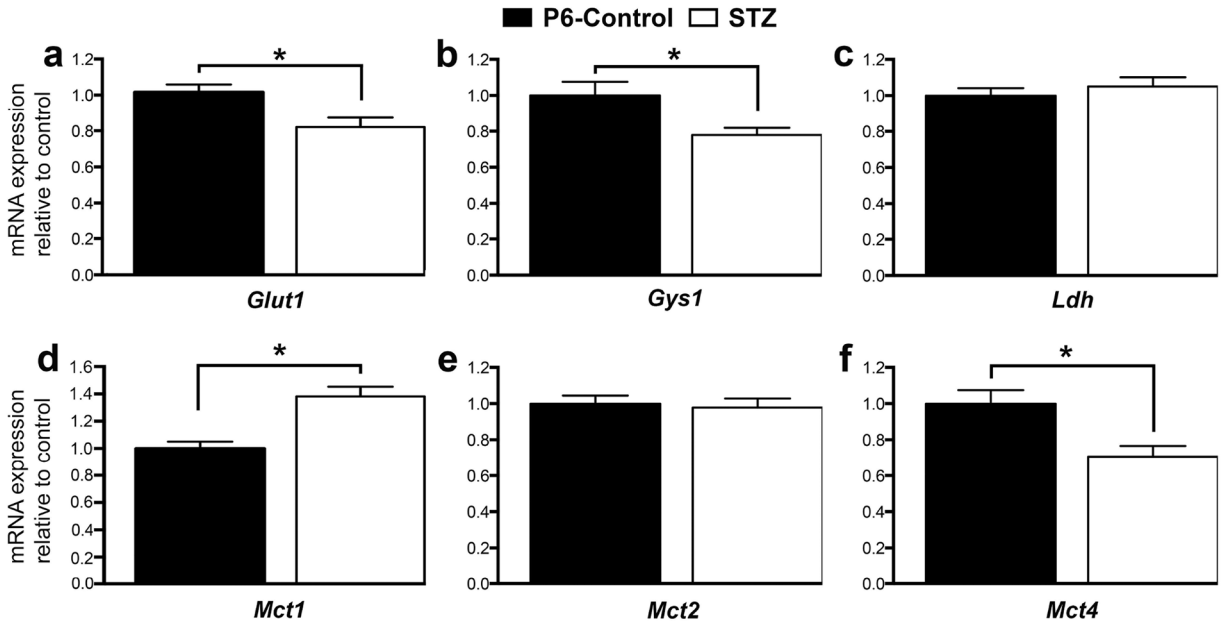

Figure 4.

mRNA expression of selected genes in the P6-Control (black) and STZ (white) groups. Values are mean ± SEM normalized to the P6-Control group; N = 8 per group. *p < 0.05. Abbreviations: *Glut1*, glucose transporter 1; *Gsy1*, glycogen synthase 1; *Ldh*, lactate dehydrogenase; *Mct1*, monocarboxylate transporter 1; *Mct2*, monocarboxylate transporter 2; *Mct4*, monoscarboxylate transporter 4.